Automated Caries Detection using a 3D Intraoral Scanner. An in Vivo Validation Study

Stavroula Michou (stmi@sund.ku.dk)
University of Copenhagen
Mathias S. Lambach
3Shape TRIOS A/S
Panagiotis Ntovas
National and Kapodistrian University of Athens
Ana R. Benetti
University of Copenhagen
Azam Bakhshandeh
University of Copenhagen
Christos Rahiotis
National and Kapodistrian University of Athens
Kim R. Ekstrand
University of Copenhagen
Christoph Vannahme
3Shape TRIOS A/S

Research Article

Keywords: Caries Detection, Intraoral Scanner, periodontal diseases

Posted Date: June 10th, 2021

DOI: https://doi.org/10.21203/rs.3.rs-590542/v1

Automated caries detection using a 3D intraoral scanner. An *in vivo* validation study.

Stavroula Michou[1,2*], Mathias S. Lambach[2,+], Panagiotis Ntovas[3,+], Ana R. Benetti[1], Azam Bakhshandeh[1], Christos Rahiotis[3], Kim R. Ekstrand[1], and Christoph Vannahme[2]

[1]University of Copenhagen, Department of Odontology, 2200 Copenhagen, Denmark
[2]3Shape TRIOS A/S, 1060 Copenhagen, Denmark
[3]National and Kapodistrian University of Athens, School of Dentistry, 11527 Athens, Greece
[*]corresponding author, stmi@sund.ku.dk
[+]these authors contributed equally to this work

ABSTRACT

The use of 3D intraoral scanners (IOS) and software that can support automated detection and objective monitoring of oral diseases such as caries, tooth wear or periodontal diseases is increasingly receiving attention from researchers and industry. This study clinically validates an automated caries scoring system for occlusal caries detection and classification, previously developed for an IOS system featuring fluorescence (TRIOS 4, 3Shape TRIOS A/S, Denmark). Four algorithms (*ALG1, ALG2, ALG3, ALG4*) are assessed for the IOS; the first three are based only on fluorescence information, while *ALG4* also takes into account the tooth color information. The diagnostic performance of these automated algorithms is compared with the diagnostic performance of the clinical visual examination, while histological assessment is used as reference. Additionally, possible differences between *in vitro* and *in vivo* diagnostic performance of the IOS system are investigated.
The algorithms show comparable *in vivo* diagnostic performance to the visual examination. Only minor differences between their *in vitro* and *in vivo* diagnostic performance are noted. This novel IOS system exhibits encouraging performance for clinical application on occlusal caries detection and classification. Different approaches can be investigated for possible optimization of the system.

Introduction

The use of 3D intraoral scanners (IOS) and corresponding software for oral disease detection and monitoring has proven potential[1–5]. There is increasing development in this area, both by companies that produce medical devices, and by researchers seeking improved devices and software that can support automated detection and objective monitoring of oral diseases such as caries, tooth wear and periodontal diseases either in a clinical setup or remotely[1–12].

In a previous study, we investigated the implementation and diagnostic performance of an automated caries scoring system based on the fluorescence method using blue-violet light (415 nm wavelength) in a 3D IOS system (TRIOS 3, 3Shape TRIOS A/S, Denmark)[1]. Different caries classification algorithms were investigated for this fluorescence-based IOS system, showing good *in vitro* diagnostic performance when assessing occlusal caries lesions. More specifically, at the caries stages where the comparison between the conventional methods and the IOS caries classification system was possible, the best-performing IOS algorithms employing optimal cut-offs showed slightly higher sum of Sensitivity (SE) and Specificity (SP) (SE+SP = 1.58-1.84) than the visual-tactile examination (SE+SP = 1.73-1.81) and significantly higher than the radiographic examination (SE+SP = 1.37-1.78). The only exception was observed for the caries lesions located in the outer third of dentin, where the radiographic assessment showed a higher value (SE+SP = 1.78) compared to the best-performing IOS algorithms (SE+SP = 1.67-1.69). In that study, both visual-tactile and radiographic assessments employed the International Caries Detection and Classification System criteria (ICDAS)[1,13]. The idea behind the development of the automated caries detection and classification system to accompany the 3D IOS is that by combining a method similar to the well-documented Quantitative Light-Induced Fluorescence (QLF)[6,8,14,15] with the 3D information provided by the IOS, detection and monitoring of the caries lesions can potentially be improved.

The study mentioned above[1] and later investigations led to the development of different algorithms for an automated caries scoring system, and its implementation in a prototype software accompanying the 3D IOS (TRIOS 4, 3Shape TRIOS A/S, Denmark). These algorithms employ red and green fluorescence (R_{fluo}, G_{fluo}) signal[1] resulting from scanning with light at 415 nm. However, tooth color (Red, Green and Blue) signal (*R, G, B*) is simultaneously obtained from scanning the teeth with white light. It is speculated that by combining all the available color information on a 3D model, and by analyzing any difference of color signal intensity on the tooth surface together with the fluorescence changes corresponding to sound and demineralized

dental tissue, the accuracy in detecting occlusal caries lesions could be increased[12,16,17]. This hypothesis is supported by previous research, in which similar approaches combining the fluorescence method with reflectance enhancement showed relatively accurate detection and monitoring of caries lesions *in vitro* (SE+SP = 1.55)[16,17]. Thus, an algorithm combining all the color information on the 3D model (R_{fluo}, G_{fluo}, *R, G, B*) was developed and tested on existing sample[1]. This specific algorithm showed the best *in vitro* diagnostic performance for occlusal caries detection and classification at one optimal cut-off in enamel and two in dentin (area under the ROC curve, $A_z > 0.9$, SE > 0.83 and SP > 0.87), which motivated us to include it in this validation study.

Based on the diagnostic performance of the 3D IOS for *in vitro* occlusal caries detection[1] and considering the unique advantage of 3D models, which combine geometry, color signal from the tissues, and, in this case, fluorescence signal, we assume that this device can help to overcome some limitations observed for the existing 2D intraoral cameras featuring fluorescence for caries detection. For example, difficulties in obtaining reproducible 2D intraoral images for monitoring caries lesions over time is a common issue, limited largely by the image acquisition angle. The latter can significantly affect the size of the lesion depicted on the 2D images[18] but is expected to have less influence on the assessment using 3D models where the averaging of image data gives less noise and eliminates images obtained from steep angles.

Despite the good results obtained for the IOS system in the previous *in vitro* study, it was essential to validate the algorithms and corresponding cut-offs developed on a new blind sample *in vivo*[19]. Previous studies assessing other devices featuring fluorescence for caries detection have observed significant differences among the devices' *in vitro* diagnostic performance at optimal cut-offs and their subsequent performance achieved in *in vivo* validation studies, where pre-defined cut-offs were assessed on independent samples[19–22]. The latter has led previous researchers to the conclusion that the *in vitro* developed cut-offs need modification for *in vivo* application.

Aim

The purpose of this study was to clinically validate four automated caries scoring system algorithms previously developed for the IOS system using histological assessment as reference method. Further aims were: *i)* to compare the performance of the automated scoring system with the clinical examination employing the ICDAS criteria; and *ii)* to assess possible differences in the performance of the automated system under *in vitro* and *in vivo* conditions.

Materials and Methods

Study Sample

Sample size calculation was done using the formula described by Burderer[23], for a confidence interval at 95%, absolute error at 0.1, and based on the expected diagnostic performance for the IOS system (SE ≥ 0.84, SP ≥ 0.76)[1]. This resulted in a minimum of 100 examination sites that should be included in the current study.

Permanent molars and premolars scheduled for extraction at the surgery department of the School of Dentistry of the University of Copenhagen were considered for inclusion in the study. The age range of patients was from 18 to 60 years old. Teeth with severe developmental defects, calculus on the occlusal surface, visible extensive caries lesions on other surfaces than the occlusal, and restored teeth were not included in the sample. According to these criteria, 58 teeth scheduled for extraction were selected for examination.

Ethics

This study received ethical approval from the Research Ethics Committee of the School of Dentistry of the National and Kapodistrian University of Athens (prot. nr. 423/08.07.2019) and was conducted in accordance to the declaration of Helsinki and General Data Protection Regulation (GDPR). All study participants gave informed consent and agreed to publish anonymized information or images in an online publication.

Study Design

The overall study workflow is presented in Figure 1.

This *in vivo* study with *in vitro* validation assessed four different algorithms (*ALG1-ALG4*) implemented in the IOS system for automated caries detection and classification. 3D models of the examined teeth were obtained both *in vivo* and *in vitro*, i.e. before and after tooth extraction, in order to assess any possible differences in the algorithms' performance in different conditions. The latter could potentially help draw some conclusions regarding the validity of the previous *in vitro* study assessing this 3D IOS system for caries detection, and the *in vivo* applicability of *in vitro* results. Additionally, a visual-tactile examination using the ICDAS criteria[24] was conducted *in vivo* and histological assessment was used as reference test *in vitro* (Table 1). Information regarding the examiners' calibration and blinding are provided in the supplementary material.

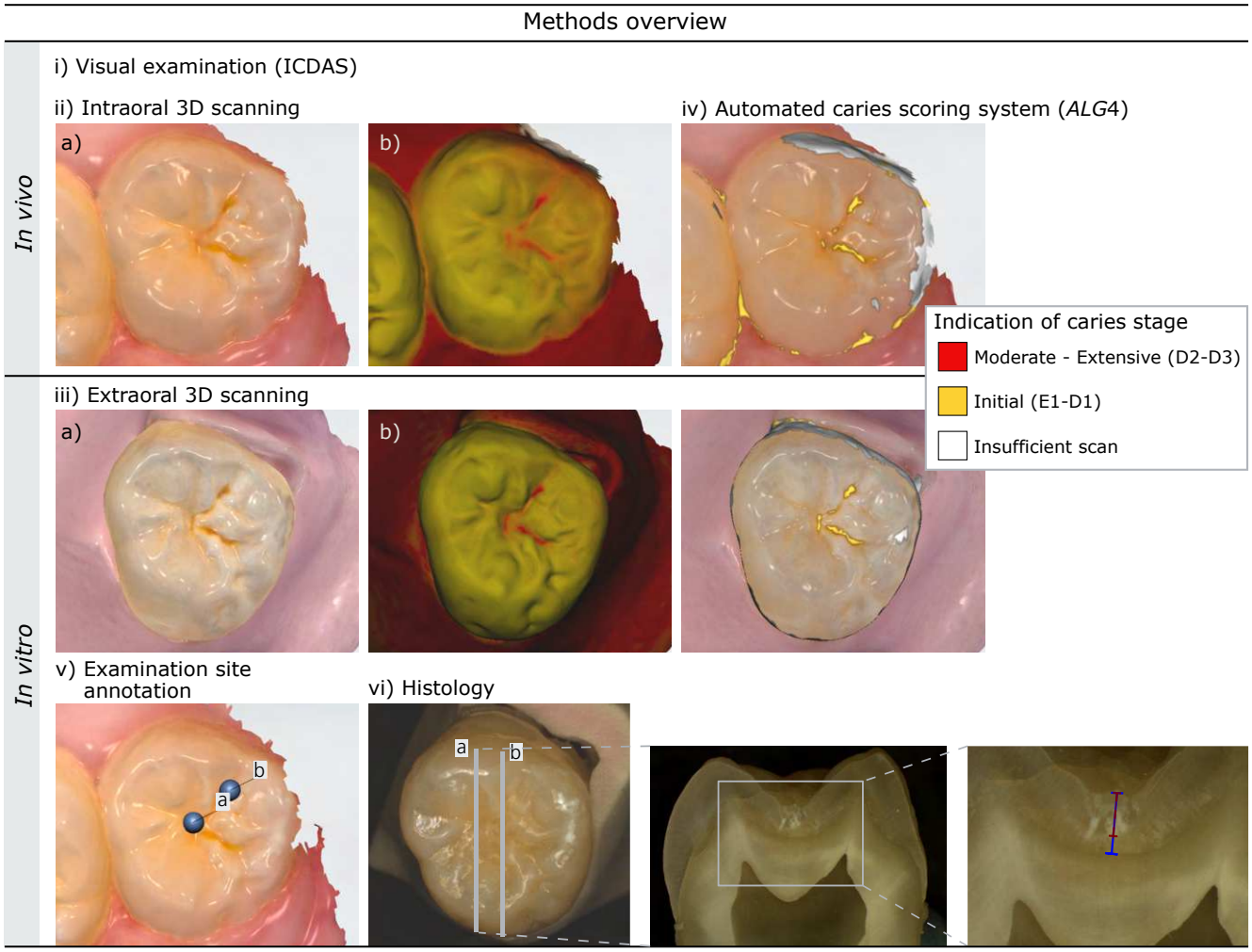

Figure 1. Study methods overview *in vivo* and *in vitro*. 3D models of the same tooth scanned iia) *in vivo* and iiia) *in vitro* using white light; the tooth color signal was mapped onto the models. The same tooth was scanned iib) *in vivo* and iiib) *in vitro* with the 415 nm wavelength light, which excites fluorescence from the dental tissues. iv) caries score indication based on TRIOS patient monitoring software (3Shape TRIOS A/S, Denmark) according to *ALG4*. Indication of caries stages: Initial; caries lesions in enamel and outer third of dentin (Histology E1-D1). Moderate-extensive; caries lesions in middle and inner thirds of dentin (Histology D2-D3). Insufficient scan: insufficient data on tooth color and/or fluorescence that does not allow the automated caries score calculation. v) selected examination sites (a, b) annotated on the 3D model. vi) tooth sectioning lines corresponding to the examination sites (a, b) for the histological assessment. On the tooth section, the red measurement line corresponds to the demineralization depth and the blue measurement line corresponds to the enamel thickness.

Visual Examination (ICDAS)

The clinical examiner (P.N.) defined one to three examination sites in the occlusal pits and fissures of each selected tooth and examined all teeth *in vivo* employing the visual ICDAS criteria for caries classification[13,25,26]. Examination was performed on dry surfaces, under proper illumination and after polishing of the occlusal surfaces with prophylactic brushes and a low-speed handpiece (Kavo Intra 20k). One score (ICDAS0-ICDAS6) was assigned to each examination site, and after the 3D model acquisition, the exact position of the examination site was annotated on the 3D model Figure 1, *v*.

3D Scanning

Subsequent to visual examination, all teeth were scanned *in vivo* using the 3D IOS TRIOS 4 (3Shape TRIOS A/S, Denmark) aided by commercial software (TRIOS and Dental Desktop, 3Shape TRIOS A/S, Denmark) and according to the manufacturer's recommendations: the dental lamp was switched off, other external light was limited as much as possible[27], teeth surfaces were clean and dry and the recommended scanning strategy was followed.

First, by scanning with white light, a digital 3D model of the teeth with tooth color texture was created (Figure 1, *iia*). Then, by scanning a second time using light at 415 nm, a texture representing the fluorescence signal received from the tissues was mapped onto the 3D model (Figure 1, *iib*). The intraoral scanning procedure was finalized when sufficient tooth color and fluorescence information was obtained according to the software's indication.

Following *in vivo* intraoral scanning, the teeth were extracted and transferred shortly thereafter to the laboratory for *in vitro* scanning. There, the teeth were mounted on individual bases made of putty impression material (Zetalabor, Zhermack, Italy) and scanned again with the same IOS system, following the same procedures described for the intraoral scanning *in vivo*. The *in vitro* models were obtained in a dark room (Figure 1, *iiia, b*).

Intraoral Scanner's Algorithms

Four different algorithms (*ALG1-ALG4*) developed for caries detection and classification on the 3D models were assessed. An article describing the development of the first three algorithms (*ALG1-ALG3*) was published previously by Michou et al.[1]. Mathematical functions f_2-f_4 of the mentioned study correspond to *ALG1-ALG3* in the current study. The last algorithm, *ALG4*, was developed at a later stage using the same sample and methods as described in the above mentioned study[1]. Histology was used as the reference method for the development of all algorithms. Receiver Operating Characteristic (ROC) analyses were conducted on the raw data from each algorithm. Optimal cut-offs for different caries severity levels according to histology were defined by the sum of SE and SP at each histological level (Table 1).

For *ALG1* and *ALG2*, reliable independent cut-offs (SE+SP $>$ 1.7) could only be defined for two caries severity levels: *i)* caries lesions in enamel ($\geq$ E1) and *ii)* caries lesions in dentin ($\geq$ D1). For *ALG3* and *ALG4*, an additional cut-off corresponding to *iii)* caries lesions in the middle-inner third of dentin ($\geq$ D2) was also defined. Thus, using *ALG3* and *ALG4* the lesions in the outer third of dentin received a different score than the lesions in the middle-inner third (Table 1). The first three algorithms (*ALG1-ALG3*) were based exclusively on the fluorescence signal received by the dental tissues. More specifically: *ALG1* represents the absolute green fluorescence signal (G_{fluo}) on each examination site; *ALG2* represents again the G_{fluo} but taking as reference the average G_{fluo} from the sound surfaces on the same tooth; and *ALG3* represents both red (R_{fluo}) and green fluorescence signal G_{fluo} on the examination sites and uses as reference the average R_{fluo} and G_{fluo} from sound surfaces located on the same tooth. The last algorithm, *ALG4*, was found by logistic regression, and takes into account both fluorescence (R_{fluo}, G_{fluo}) and tooth color signal (R, G, B) from the examination sites using the sound tooth surfaces as reference.

Rather than selecting the areas of interest manually in order to calculate the caries scores[1], in the current study the prototype software already integrated the algorithms *ALG1-ALG4*. This software was based on the commercially-available TRIOS Patient Monitoring software (3Shape TRIOS A/S, Denmark) and enabled the automated display of a color overlay on the 3D models of the teeth, which represented the caries severity indication on the model according to each algorithm (Figure 1, *iv*).

Using this custom-made software, an independent examiner not involved in the clinical examination (S.M.) assessed the 3D models acquired both *in vivo* and *in vitro*. The automated scores given from each algorithm on the 3D models were registered on the same examination sites initially selected by the clinical examiner (P.N.). The scoring system corresponding to each algorithm is shown in Table 1.

Reference test - Histology

Histological assessment was used as the reference standard such as that described in a previous study[1]. The maximum caries lesion depth, as well as the enamel or dentin thickness (at the same position), were registered for each examination site (Figure 1, *vi*). Based on the outcome resulting from the fraction caries lesion depth/enamel thickness or caries lesion depth/dentin thickness for lesions located in enamel and dentin, respectively, the following histological scores were given to each examination site:

- E0 sound;
- E1 lesions in the outer half of enamel (fractions $<$ 0.5);
- E2 lesions in the inner half of enamel including the dentin-enamel junction (DEJ) (fractions $\geq$ 0.5);

– D1 lesions in the outer third of dentin (fractions < 0.33),
– D2 lesions in the middle third of dentin (fractions ≥ 0.33 and < 0.66); and
– D3 lesions in the inner third of dentin, with or without pulp involvement (fractions ≥ 0.66).

	Histology	*ALG1,2*	*ALG3,4*	Visual (ICDAS)
SOUND	**E0:** Sound	**0**	**0**	**0:** Sound tooth surfaces show no visible evidence of caries when viewed after cleaning and after 5 seconds of air-drying.
ENAMEL	**E1:** Caries in the outer half of enamel	**1**	**1**	**1:** First visual change in enamel (opacity or discoloration) visible at the entrance of pit or fissure, seen after 5 seconds of air-drying.
	E2: Caries in the inner half of enamel – including the dentin-enamel junction (DEJ)			**2:** Distinct visual change in enamel (opacity or discoloration) visible when both wet and dry, with no evidence of surface breakdown or underlying dentin shadowing.
DENTIN	**D1:** Caries in the outer third of dentin		**2**	
	D2: Caries in the middle third of dentin	**2**	**3**	**3:** A white or brown spot lesion with localized enamel breakdown, without visible dentine exposure.
				4: Non-cavitated surface with an underlying dentine shadow, which obviously originated on the surface being evaluated
	D3: Caries in the inner third of dentin			**5:** Visually distinct cavity in opaque or discoloured enamel and exposed dentine.
				6: Extensive (more than half of the surface) and visually distinct cavity with exposed dentine.

Table 1. Scoring systems employed by the different methods according to histology.

Data Analysis

All examination sites were assigned an independent score using the different software algorithms, visual assessment (ICDAS), and histology.

Spearman's rank correlation coefficient (r_s) was used to assess possible correlation between the histology and the scores originated from algorithms or visual assessment. The diagnostic performance for all methods was expressed by ROC analyses and contingency tables using histology as reference (see Supplementary table S1). Area under the ROC curve (Az), Sensitivity (SE), Specificity (SP) and accuracy (ACC) were then calculated after dichotomizing the data at the E1, D1 and D2 histological levels, which correspond to the three cut-offs defined for the algorithms. Areas under the ROC curves for the investigated methods at the E1, D1 and D2 levels were compared pairwise using DeLong's algorithm[28], while SE and SP values were compared using McNemar's test[29]. The standard error (Std. Err.) for SE and SP was adjusted for possible clustering effect as multiple examination sites were selected on the same tooth[30–32]. The McNemar-Bowker test was employed to assess possible differences between the *in vivo* and *in vitro* results for the different algorithms.

Spearman's rank correlation coefficient, contingency tables ROC analyses, and McNemar's test were performed using IBM SPSS Statistics (Version 26, IBM Corporation). Other calculations were performed in Excel (Microsoft Office 2016) and comparison of areas under ROC curves was made using MedCalc statistical software (Version 19.6.4, MedCalc Software Ltd, Belgium). Confidence level was defined at 95% for all statistical tests.

Results

Out of the 58 teeth initially included for examination, 5 either did not fulfill the study's inclusion criteria after tooth extraction and second inspection *in vitro*, or were destroyed while sectioning for histological analysis. Finally, a total number of 53 teeth

with 118 examination sites were included for statistical analysis. Out of those, some examination sites could not be assessed using the algorithms, either due to insufficient scan data or algorithm failure; the number of missing examination sites for each algorithm can be seen in the contingency tables (Supplementary table S1). According to histology, out of the total number of examination sites ($n = 118$), 28 were sound (E0), 51 were initial caries lesions in enamel (E1, E2), 31 were lesions in the outer third of dentin (D1) and only 8 were lesions located in the middle-inner third of dentin ($\geq$ D2).

Diagnostic performance

Table 2 shows descriptive results including correlation to the histological scores (r_s), Az, SE, SP, ACC and SE+SP for all algorithms, both *in vivo* and *in vitro*, and for visual examination *in vivo*. Figure 2 presents the ROC curves corresponding to algorithms and visual examination *in vivo*. All methods resulted in significant correlation (r_s) with histology ($p < 0.001$):

		(a) In vivo				
		ALG1	*ALG2*	*ALG3*	*ALG4*	Visual
	r_S	0.37 (0.08)	0.39 0.08)	0.50 0.08)	0.46 (0.08)	0.54 (0.07)
$\geq$E1	Az	0.71 (0.06)*	0.75 (0.05)*	0.78 (0.05)*	0.71 (0.06)*	0.76 (0.06)*
	SE	$0.74(0.05)^{AB}$	$0.70(0.05)^{B}$	$0.56(0.06)^{C}$	$0.71(0.05)^{AB}$	$0.82(0.03)^{A}$
	SP	$0.53(0.03)^{B}$	$0.59(0.02)^{B}$	$1.00(0.00)^{A}$	$0.59(0.03)^{B}$	$0.59(0.04)^{B}$
	ACC	0.70	0.68	0.63	0.69	0.79
	SE+SP	1.27	1.28	1.56	1.30	1.41
$\geq$D1	Az	0.73 (0.06)*	0.70 (0.06)*	0.81 (0.06*)	0.83 (0.06)*	N/A
	SE	0.89 (0.10)*	0.71 (0.16)*	0.67 (0.12)*	0.78 (0.13)*	N/A
	SP	$0.55(0.03)^{C}$	$0.62(0.02)^{B}$	$0.91(0.02)^{A}$	$0.88(0.02)^{A}$	N/A
	ACC	0.61	0.63	0.87	0.86	N/A
	SE+SP	1.45	1.32	1.58	1.65	N/A
$\geq$D2	Az	N/A	N/A	0.81 (0.08)*	0.90 (0.04)*	0.90 (0.04)*
	SE	N/A	N/A	0.73 (0.15)*	0.91 (0.19)*	0.93 (0.07)*
	SP	N/A	N/A	$0.88(0.02)^{A}$	$0.86(0.02)^{A}$	$0.75(0.02)^{B}$
	ACC	N/A	N/A	0.86	0.87	0.77
	SE+SP	N/A	N/A	1.60	1.77	1.68

		(b) In vitro			
		ALG1	*ALG2*	*ALG3*	*ALG4*
	r_S	0.37 (0.08)	0.20 (0.09)	0.41 (0.08)	0.47 (0.08)
$\geq$E1	Az	0.70 (0.08)*	0.70 (0.08)*	0.70 (0.06)*	0.76 (0.05)*
	SE	$0.85(0.03)^{A}$	$0.81(0.03)^{A}$	$0.59(0.05)^{B}$	$0.80(0.04)^{A}$
	SP	0.53 (0.03)*	0.59 (0.03)*	0.71 (0.02)*	0.59 (0.03)*
	ACC	0.80	0.77	0.60	0.77
	SE+SP	1.38	1.39	1.29	1.39
$\geq$D1	Az	$0.73(0.05)^{A}$	$0.58(0.07)^{B}$	$0.81(0.06)^{A}$	$0.83(0.05)^{A}$
	SE	$1.00(0.00)^{A}$	$0.47(0.16)^{B}$	$0.72(0.13)^{AB}$	$0.74(0.12)^{AB}$
	SP	$0.46(0.02)^{C}$	$0.58(0.02)^{B}$	$0.86(0.02)^{A}$	$0.81(0.02)^{A}$
	ACC	0.55	0.56	0.84	0.72
	SE+SP	1.46	1.05	1.58	1.54
$\geq$D2	Az	N/A	N/A	0.85 (0.05)*	0.85 (0.05)*
	SE	N/A	N/A	0.82 (0.14)*	0.83 (0.12)*
	SP	N/A	N/A	0.83 (0.02)*	0.83 (0.02)*
	ACC	N/A	N/A	0.83	0.83
	SE+SP	N/A	N/A	1.65	1.66

Table 2. Descriptive results for all methods assessed *in vivo* (a) and *in vitro* (b). r_s, Spearman's rank correlation coefficient; Az, area under the ROC curve; SE, sensitivity; SP, specificity; ACC, diagnostic accuracy; N/A, not available. Standard error is provided in parenthesis. SE and SP standard error is adjusted for clustered data[32]. The significant differences within the same row are marked with capital letters following the sequence $A > B > C$. *Indicates no significant differences in the specific row of data. Confidence level was defined at 95% for all statistical tests.

ALG3, *ALG4* and visual assessment showed moderate correlation ($0.41 \leq r_S \leq 0.54$) and *ALG1* and *ALG2* showed fair or weak

correlation ($r_S < 0.40$) Table 2.

Caries detection level (Histology $\geq$ E1)

When assessing the ability of the different investigated methods to detect caries lesions *in vivo* and *in vitro* (Histology $\geq$ E1), all methods resulted in similar area under the ROC curves (Az); no significant differences among the Az values of different methods were observed ($p > 0.05$). The highest SE and ACC were exhibited by *ALG1*, *ALG4*, and visual assessment, while significantly lower SE was found for *ALG3* ($p < 0.001$). However, *ALG3* presented the highest SP ($p < 0.05$) as well as the highest sum of SE and SP *in vivo*. No significant differences among SP values were observed *in vitro*.

Caries in dentin (Histology $\geq$ D1)

As regards the detection and classification of caries lesions in the outer third of dentin (Histology $\geq$ D1), both *in vitro* and *in vivo*, only the IOS algorithms were assessed as there is no ICDAS score for visual examination that can reliably distinguish between lesions in enamel and initial lesions in the outer third of dentin[24]. When assessing the 3D models acquired *in vivo*, no significant difference among the Az for all algorithms was detected ($p > 0.05$). However, regarding measurements on models obtained *in vitro*, *ALG2* resulted in significantly lower Az values than *in vivo* ($p < 0.01$). *ALG3* and *ALG4* showed the highest Az, SP, ACC, and sum of $SE + SP$ both *in vitro* and *in vivo*. On the other hand, *ALG*1 exhibited significantly lower SP ($p < 0.05$) than all the other algorithms, but high SE.

Caries in the middle-inner third of dentin (Histology $\geq$ D2)

In the middle - inner third of dentin (Histology $\geq$ D2), only the *in vivo* visual scores, and those from *ALG3* and *ALG4* were assessed. Regarding the Az and SE values, no significant differences among the different methods were observed. Visual assessment showed the lowest ACC and SP *in vivo*, with the latter being significantly inferior to the SP of *ALG3* and *ALG4*. Almost identical *in vitro* diagnostic performance was observed for *ALG3* and *ALG4*.

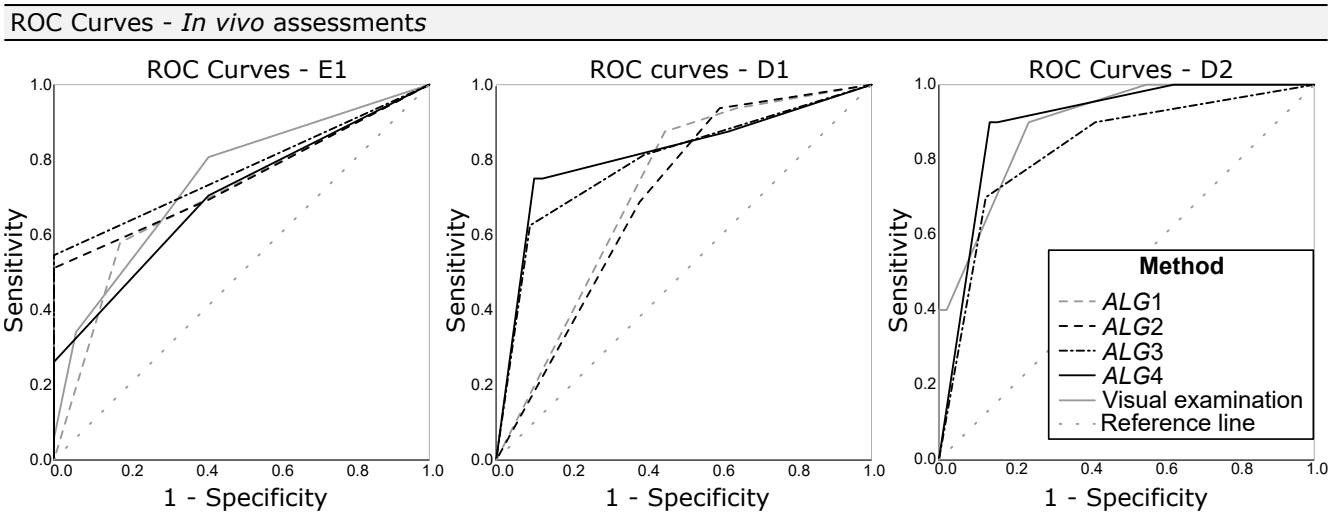

Figure 2. ROC curves corresponding to the four algorithms (*ALG1-ALG4*) and visual assessment investigated *in vivo* at the histological levels E1, D1, D2.

Algorithm reproducibility *in vivo* vs. *in vitro*

No significant difference was found between *in vivo* and *in vitro* ordinal scores resulting from the IOS algorithms (McNemar Bowker test, $p > 0.05$). In addition, for all algorithms and at all assessed histological levels (E1, D1, D2), no significant difference was detected between the Az values obtained from *in vivo* or *in vitro* assessments ($p > 0.05$).

However, as regards the caries detection level (Histology $\geq E1$), *ALG1*, *ALG2*, and *ALG4* showed higher SE *in vitro* than *in vivo* (McNemar's test on binary data: *ALG1,2* $p < 0.01$, *ALG4* $p = 0.04$).

Discussion

The algorithms for automated caries detection and classification developed for the IOS system (TRIOS 4, 3Shape TRIOS A/S, Denmark) were validated against histology. When considering the detection and classification of initial (Histology $\geq$ E1) and moderate-extensive caries lesions (Histology $\geq$ D2), the IOS algorithms showed diagnostic performance comparable to visual

examination using ICDAS criteria; these results are in agreement with the literature assessing the QLF method[14,21]. This is a significant step towards implementing an automated caries scoring system in a commercial 3D IOS system, which can aid caries detection and potentially support caries monitoring in everyday clinical practice.

However, as expected in the current study and as also seen in the literature during validation of cut-offs defined for other devices[19–21], the diagnostic performance of the investigated algorithms was considerably inferior to the one observed at optimal cut-offs defined in a previous *in vitro* study[1]. This agrees with previous studies supporting that no absolute cut-offs can be defined for the devices featuring optical caries detection with fluorescence. The developed cut-offs can only be used as an indication for the relative caries lesion depth[19–22].

No significant overall difference was detected regarding the performance of the algorithms on the 3D models obtained *in vivo* or *in vitro*. This finding confirms that future caries validation studies assessing this IOS system can be conducted *in vitro* and provide a good indication of the *in vivo* diagnostic performance. Subsequently, caries classification cut-offs defined *in vitro* can potentially be applied *in vivo*. However, a prerequisite is that appropriate methodological procedures are followed *in vitro* after the tooth extraction, e.g. short storage period in liquid or freezing of teeth to avoid the diffusion of porphyrins in the storage solution[33], fluorescence image acquisition in a dark room to avoid the effect of external light[27].

Some limitations are identified regarding the sample in this study. The fact that the investigated teeth were scheduled for extraction means that the majority were third molars, in some cases semi-erupted, or with large cavities. In addition, a few teeth were extracted for orthodontic reasons, or due to periodontal problems. The automated caries detection system is mainly intended to be used on permanent posterior teeth with initial to moderate caries lesions, for which monitoring can evaluate the progression or regression of the lesions, as well as the effectiveness of preventive measures. Thus, the constitution of the sample in the current study was not fully representative of the teeth in a clinical scenario. Nevertheless, this is an inherent limitation that, due to ethical considerations, could not be avoided in a validation study like this, where extraction and *in vitro* histological assessment were carried out.

Furthermore, the inclusion of third molars and semi-impacted teeth of limited clinical access created additional limitations, for example insufficient cleaning of the occlusal surface in some cases. Considering that the dental biofilm can emit strong red-orange fluorescence signal[34,35], good cleaning of teeth is essential to assess caries lesions with the fluorescence method. Otherwise, the fluorescence signal from bacteria might lead to false indications by devices assessing fluorescence. This phenomenon became apparent in this study due to differences observed in red fluorescence texture when assessing the scans of the same teeth obtained *in vitro* and *in vivo* (Figure 1, iib versus iiib). This variation in fluorescence signal resulted in higher SE values *in vitro* for the E1 histological level (*ALG1, ALG2, ALG4*). Additionally, in some cases, due to limited access of the scanner to third molars *in vivo*, areas of insufficient 3D scanning data (Figure 1, vi) on the occlusal surfaces were noted, thus leading to failure of the automated caries scoring algorithms. This is expected to be observed in a clinical setup as well, and the operators should be aware of such limitations.

Despite the good performance of IOS algorithms for caries detection and classification, there is still possibility for future algorithm improvement and implementation of other parameters, such as the surface area of caries lesions, in order to improve diagnostic performance. Incorporating the lesion surface area in the algorithms can potentially prevent the false classification of some narrow initial arrested caries lesions as more extensive lesions due to dark stains. There may also be potential in the assessment of caries lesion activity using this system by examining red fluorescence from the dental plaque, estimating lesion size change over time (i.e. monitoring), and obtaining information on surface roughness[36], all worth investigating[37]. Lastly, the development of advanced algorithms based on machine learning seems promising given the recent advances in this field[9,10,12].

Conclusion

The automated algorithms for occlusal caries detection and classification accompanying the IOS system were validated against histology, showing an overall comparable *in vivo* diagnostic performance to the visual examination. The algorithms can be used both for *in vitro* and *in vivo* assessments. Only minor differences between their *in vitro* and *in vivo* diagnostic performance were noted. This novel system exhibits encouraging performance for clinical application on occlusal caries detection and classification, while different approaches can be investigated for potential optimization of the system.

References

1. Michou, S. *et al.* Development of a fluorescence-based caries scoring system for an intraoral scanner: An in vitro study. *Caries Res.* **54**, 324–335, DOI: 10.1159/000509925 (2020).
2. Michou, S., Vannahme, C., Ekstrand, K. & Benetti, A. Detecting early erosive tooth wear using an intraoral scanner system. *J. Dent.* **100**, 103445, DOI: 10.1016/j.jdent.2020.103445 (2020).
3. Zhang, J., Huang, Z., Cai, Y. & Luan, Q. Digital assessment of gingiva morphological changes and related factors after initial periodontal therapy. *J. Oral Sci.* **63**, 59–64, DOI: 10.2334/josnusd.20-0157 (2021).

4. Chen, Q., Jin, X., Zhu, H., Salehi, H. S. & Wei, K. 3D distribution of dental plaque on occlusal surface using 2D-fluorescence-image to 3D-surface registration. *Comput. Biol. Med.* **123**, 103860, DOI: 10.1016/j.compbiomed.2020.103860 (2020).
5. El-Sharkawy, Y. H. & Elbasuney, S. Laser induced fluorescence with 2-D Hilbert transform edge detection algorithm and 3D fluorescence images for white spot early recognition. *Spectrochim. Acta Part A Mol. Biomol. Spectrosc.* **240**, 118616, DOI: 10.1016/j.saa.2020.118616 (2020).
6. Pretty, I. A. & Ellwood, R. P. The caries continuum: Opportunities to detect, treat and monitor the re-mineralization of early caries lesions. *J. Dent.* **41**, S12–S21, DOI: 10.1016/j.jdent.2010.04.003 (2013).
7. Estai, M., Bunt, S., Kanagasingam, Y., Kruger, E. & Tennant, M. Diagnostic accuracy of teledentistry in the detection of dental caries: A systematic review. *J. Evid. Based. Dent. Pract.* **16**, 161–172, DOI: 10.1016/j.jebdp.2016.08.003 (2016).
8. Fried, D. Optical methods for monitoring demineralization and caries. In Wilder-Smith, P. & Ajdaharian, J. (eds.) *Oral Diagnosis*, 1–27, DOI: 10.1007/978-3-030-19250-1 (Springer International Publishing, Cham, 2020), 1st edn.
9. Schwendicke, F., Samek, W. & Krois, J. Artificial intelligence in dentistry: Chances and challenges. *J. Dent. Res.* **99**, 769–774, DOI: 10.1177/0022034520915714 (2020).
10. Schwendicke, F., Elhennawy, K., Paris, S., Friebertshäuser, P. & Krois, J. Deep learning for caries lesion detection in near-infrared light transillumination images: A pilot study. *J. Dent.* **92**, DOI: 10.1016/j.jdent.2019.103260 (2020).
11. Patil, S., Kulkarni, V. & Bhise, A. Algorithmic analysis for dental caries detection using an adaptive neural network architecture. *Heliyon* **5**, e01579, DOI: 10.1016/j.heliyon.2019.e01579 (2019).
12. Berdouses, E. D. *et al.* A computer-aided automated methodology for the detection and classification of occlusal caries from photographic color images. *Comput. Biol.* **62**, 119–135, DOI: 10.1016/j.compbiomed.2015.04.016 (2015).
13. Ekstrand, K. R., Gimenez, T., Ferreira, F. R., Mendes, F. M. & Braga, M. M. The International Caries Detection and Assessment System-ICDAS: A Systematic Review. *Caries Res.* **52**, 406–419, DOI: 10.1159/000486429 (2018).
14. Pretty, I. A. Caries detection and diagnosis: Novel technologies. *J. Dent.* **34**, 727–739, DOI: 10.1016/j.jdent.2006.06.001 (2006).
15. de Josselin de Jong, E. *et al.* A new method for in vivo quantification of changes in initial enamel caries with laser fluorescence. *Caries Res.* **29**, 2–7, DOI: 10.1159/000262032 (1995).
16. Amaechi, B. T. & Ramalingam, K. Evaluation of fluorescence imaging with reflectance enhancement technology for early caries detection. *Am. J. Dent.* **27**, 112–116, DOI: 10.13140/2.1.2473.0245 (2014).
17. Xiao, Q. *et al.* Evaluation of Fluorescence Imaging with Reflectance Enhancement (FIRE) for quantifying enamel demineralization In vitro. *Caries Res.* **49**, 531–539, DOI: 10.1159/000365298 (2015).
18. Ando, M., Eckert, G. J., Stookey, G. K. & Zero, D. T. Effect of Imaging Geometry on Evaluating Natural White-Spot Lesions Using Quantitative Light-Induced Fluorescence. *Caries Res.* **38**, 39–44, DOI: 10.1159/000073919 (2004).
19. Jablonski-Momeni, A., Heinzel-Gutenbrunner, M. & Klein, S. M. In vivo performance of the VistaProof fluorescence-based camera for detection of occlusal lesions. *Clin Oral Investig* **18**, 1757–1762, DOI: 10.1007/s00784-013-1150-9 (2014).
20. Heinrich-Weltzien, R., Weerheijm, K. L., Kuhnisch, J., Oehme, T. & Stosser, L. Clinical evaluation of visual, radiographic, and laser fluorescence methods for detection of occlusal caries. *J. Dent. Child.* **69**, 127–132 (2002).
21. Jablonski-Momeni, A. *et al.* Performance of a fluorescence camera for detection of occlusal caries in vitro. *Odontology* **99**, 55–61, DOI: 10.1007/s10266-010-0139-y (2011).
22. Diniz, M. B. *et al.* The performance of conventional and fluorescence-based methods for occlusal Caries Detection: An in vivo study with histologic validation. *J. Am. Dent. Assoc.* **143**, 339–350, DOI: 10.14219/jada.archive.2012.0176 (2012).
23. Buderer, N. M. F. Statistical methodology: I. Incorporating the prevalence of disease into the sample size calculation for sensitivity and specificity. *Acad. Emerg. Med.* **3**, 895–900, DOI: 10.1111/j.1553-2712.1996.tb03538.x (1996).
24. Ekstrand, K. R. *et al.* Detection and activity assessment of primary coronal caries lesions: A methodologic study. *Oper. Dent.* **32**, 225–235, DOI: 10.2341/06-63 (2007).
25. Ismail, A. I. *et al.* The International Caries Detection and Assessment System (ICDAS): an integrated system for measuring dental caries. *Community Dent. Oral Epidemiol.* **35**, 170–178, DOI: 10.1111/j.1600-0528.2007.00347.x (2007).
26. Pitts, N. B. & Ekstrand, K. International caries detection and assessment system (ICDAS) and its international caries classification and management system (ICCMS) - Methods for staging of the caries process and enabling dentists to manage caries. *Community Dent. Oral Epidemiol.* **41**, 41–52, DOI: 10.1111/cdoe.12025 (2013).

27. Pretty, I. A., Edgar, W. M. & Higham, S. M. The effect of ambient light on QLF analyses. *J. Oral Rehabil.* **29**, 369–373, DOI: 10.1046/j.1365-2842.2002.00914.x (2002).

28. DeLong, E. R., DeLong, D. M. & Clarke-Pearson, D. L. Comparing the areas under two or more correlated receiver operating characteristic curves: A nonparametric approach. *Biometrics* **44**, 837, DOI: 10.2307/2531595 (1988).

29. Kim, S. & Lee, W. Does McNemar's test compare the sensitivities and specificities of two diagnostic tests? *Stat. Methods Med. Res.* **26**, 142–154, DOI: 10.1177/0962280214541852 (2017).

30. Jablonski-Momeni, A. *et al.* Impact of scoring single or multiple occlusal lesions on estimates of diagnostic accuracy of the visual ICDAS-II system. *Int. J. Dent.* **798283**, DOI: 10.1155/2009/798283 (2009).

31. Jablonski-Momeni, A. *et al.* Impact of measuring multiple or single occlusal lesions on estimates of diagnostic accuracy using fluorescence methods. *Lasers Med Sci* **27**, 343–352, DOI: 10.1007/s10103-011-0881-6 (2012).

32. Genders, T. S. S. *et al.* Methods for calculating sensitivity and specificity of clustered Data: A Tutorial 1. *Radiol. n Radiol.* **265**, DOI: 10.1148/radiol.12120509/-/DC1 (2012).

33. Francescut, P., Zimmerli, B. & Lussi, A. Influence of Different Storage Methods on Laser Fluorescence Values: A Two-Year Study. *Caries Res.* **40**, 181–185, DOI: 10.1159/000092223 (2006).

34. Han, S. Y., Kim, B. R., Ko, H. Y., Kwon, H. K. & Kim, B. I. Assessing the use of Quantitative Light-induced Fluorescence-Digital as a clinical plaque assessment. *Photodiagnosis Photodyn. Ther.* **13**, 34–39, DOI: 10.1016/j.pdpdt.2015.12.002 (2016).

35. Volgenant, C. M. *et al.* Red fluorescent biofilm: The thick, the old, and the cariogenic. *J. Oral Microbiol.* **8**, 1–9, DOI: 10.3402/jom.v8.30346 (2016).

36. Ando, M., Shaikh, S. & Eckert, G. Determination of caries lesion activity: Reflection and roughness for characterization of caries progression. *Oper. Dent.* **43**, 301–306, DOI: 10.2341/16-236-L (2018).

37. Novaes, T. F. *et al.* Association between quantitative measures obtained using fluorescence-based methods and activity status of occlusal caries lesions in primary molars. *Int. J. Paediatr. Dent.* **27**, 154–162, DOI: 10.1111/ipd.12242 (2017).

Acknowledgements

The authors acknowledge the laboratory technician Liselotte Larsen for her assistance with the sample storage and preparation, the development teams at 3Shape A/S for technical support, and Innovation Fund Denmark for financial support.

Author contributions statement

S.M. contributed to the study design, conducted the analyses using IOS algorithms and histology, and drafted the manuscript. M.S.L. developed the algorithm *ALG4* and implemented all the algorithms in the prototype software used in this study. P.N. collected the teeth, conducted the visual examination, and scanned the teeth using the IOS. A.R.B. coordinated the laboratory activities. A.R.B, A.B, K.R.E., C.R., and C.V. contributed in the study design. All authors reviewed and critically revised the manuscript.

Additional information

Competing interests The current study was funded by Innovation Fund Denmark (grant no. 8053-00005B). Based on the foundation's guidelines and according to an industrial PhD agreement between the industrial partner 3Shape TRIOS A/S and the University of Copenhagen, S.M. salary is partially covered by 3Shape TRIOS A/S. Furthermore, the co-authors C.V. and M.S.L. are employed at 3Shape TRIOS A/S.

The other co-authors A.R.B., A.B., C.R., P.N., and K.R.E. declare no conflicts of interest.

Figures

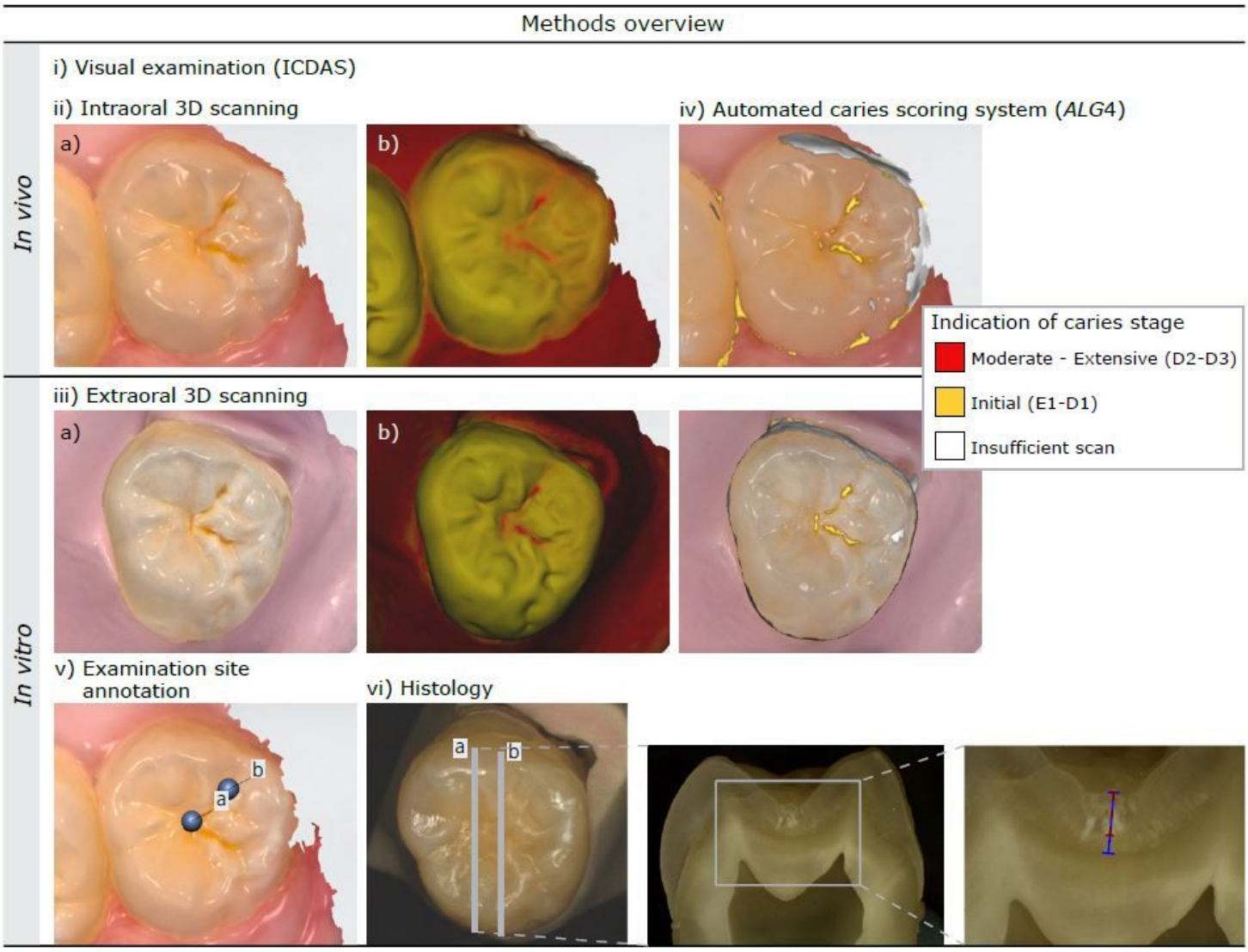

Figure 1

Study methods overview in vivo and in vitro. 3D models of the same tooth scanned iia) in vivo and iiia) in vitro using white light; the tooth color signal was mapped onto the models. The same tooth was scanned iib) in vivo and iiib) in vitro with the 415 nm wavelength light, which excites fluorescence from the dental tissues. iv) caries score indication based on TRIOS patient monitoring software (3Shape TRIOS A/S, Denmark) according to ALG4. Indication of caries stages: Initial; caries lesions in enamel and outer third of dentin (Histology E1-D1). Moderate-extensive; caries lesions in middle and inner thirds of dentin (Histology D2-D3). Insufficient scan: insufficient data on tooth color and/or fluorescence that does not allow the automated caries score calculation. v) selected examination sites (a, b) annotated on the 3D model. vi) tooth sectioning lines corresponding to the examination sites (a, b) for the histological assessment. On the tooth section, the red measurement line corresponds to the demineralization depth and the blue measurement line corresponds to the enamel thickness.

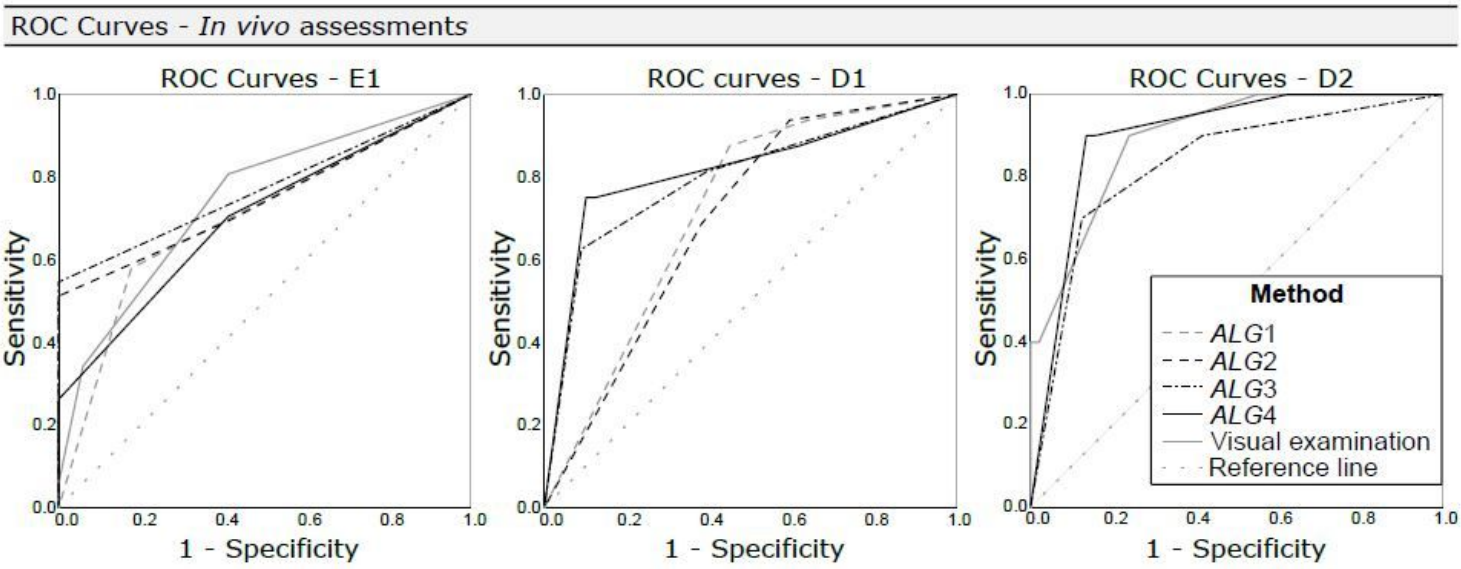

Figure 2

ROC curves corresponding to the four algorithms (ALG1-ALG4) and visual assessment investigated in vivo at the histological levels E1, D1, D2.

Supplementary Files

This is a list of supplementary files associated with this preprint. Click to download.

- SupplementarymaterialSM030621.docx
- SupplementarytableS1contingencytables030621.pdf